



### **Science Arts & Métiers (SAM)**

is an open access repository that collects the work of Arts et Métiers Institute of Technology researchers and makes it freely available over the web where possible.

This is an author-deposited version published in: <https://sam.ensam.eu>  
Handle ID: <http://hdl.handle.net/10985/17323>

#### **To cite this version :**

Imane OUTMANI, Laurence FOUILLAND-PAILLE, Jérôme ISSELIN, Mohamed EL MANSORI - Effect of Si, Cu and processing parameters on Al-Si-Cu HPDC castings - Journal of Materials Processing Technology - Vol. 249, p.559-569 - 2017

Any correspondence concerning this service should be sent to the repository

Administrator : [scienceouverte@ensam.eu](mailto:scienceouverte@ensam.eu)



# Effect of Si, Cu and processing parameters on Al-Si-Cu HPDC castings

Imane Outmani, Laurence Fouilland-Paille, Jérôme Isselin, Mohamed El Mansori

Arts et Métiers ParisTech, MSMP-EA7350, Rue Saint Dominique, BP 508, 51006 Châlons-en-Champagne, France

## A B S T R A C T

### Keywords:

High pressure die casting  
Al-Si-Cu alloys  
Tensile properties  
Hardness  
Microstructure

Chemical composition of secondary Al-Si-Cu alloys and working variables of high-pressure die casting process (HPDC) may change for the same casting parts from one country to another in the world. They can even sometimes vary from one manufacturing site to another within the same country. An experimental study on the influence of alloying elements contents (Si and Cu), casting temperature and injection pressure on mechanical properties of die cast aluminum alloys was carried out to support the automotive industry suppliers in designing their cast parts. The microstructural features and the porosity level were also investigated and assessed. The primary objective is to highlight the modification mechanisms of the achieved properties using tensile tests, hardness measurements and microstructural observations performed on a HPDC casting parts. Low pressure and low temperature increase the rate of porosity, promote the formation of coarse Fe-rich intermetallic compounds and change the morphology of  $\alpha$ -Al phases. These in turn deteriorate mechanical tensile properties. However, variation of alloying elements contents modifies the optimum properties achieved when part is made at constant casting processing parameters. Finally, the interactions between the studied parameters of HPDC and the chemical alloying elements show also a significant influence on the tensile properties.

## 1. Introduction

Among the Al-Si high-pressure die casting alloys, Al-Si-Cu alloys are the most common, they are used with different combinations of silicon and copper with other alloying elements such as magnesium and zinc. The weight percentages of chemical elements and the process parameters may vary not only from one country to another, but also from one manufacturing site to another within the same country. For example, Si content does not exceed 11 wt% in Europe (AlSi9Cu3 following EN AC 46000 standard), but up to 12 wt% in China and Japan (ADC12 following NES M3036 standard) and varies between 11 and 13 wt% in Russia (AK12M2 following Ghost 1593 standard), this variability is able to influence the mechanical properties of Al-Si-Cu alloys. However, the designs of parts produced in Europe are made on the basis of both European materials and processes but do not account this variability in the case of relocation outside of Europe. Several studies have reported the influence of alloying elements and process parameters on secondary Al-Si-Cu cast alloys, but they are mainly referred to low-pressure casting and gravity processes. Therefore, the understanding of the effects of alloying elements and processing parameters on high pressure die casting (HPDC) of Al-Si-Cu alloys in terms of mechanical properties and microstructural evolution is critical.

Following the research study of Adamane et al. (2015), most of the available literature on HPDC of Al-Si-Cu alloys investigated the

influence of injection parameters, especially the pressure, the velocity of the molten metal, the die temperature and the temperature of the molten metal parameters. According to these authors, the variation of the mechanical properties is related to the porosity and microstructural features. Concerning microstructural effect, Timelli and Bonollo (2010) noticed that the final mechanical characteristics are strictly connected to the distribution, the morphology and dimensions of primary  $\alpha$ -Al phases and eutectic Si particles, as well as to the nature of intermetallic compounds. The microstructure, in turn depends on filling process and solidification conditions. Timelli and Bonollo (2008) tried to characterize the influence of casting porosity on tensile properties of a HPDC aluminum casting. They have noticed that the amount of porosity does not affect the elastic characteristic (yield strength: YS) but decreases considerably the plastic properties (ultimate tensile strength: UTS and elongation: e%) of the material. With reference to the injection parameters of HDPC, Obiekea et al. (2014) observed that tensile yield strength and hardness increase on the contrary of porosity when high injection pressure is applied. Such mechanical characteristics were improved due to refined microstructure obtained for the applied pressures up to 140 MPa. This is confirmed by Ashiri et al. (2009) and Ashiri et al. (2014) who observed a fine microstructure with small dendrite arm spacing for high pressure. Adamane et al. (2015) reviewed the influence of injection parameters in HPDC process, particularly the injection pressure and gate velocity on the porosity and tensile

\* Corresponding author.

E-mail address: imane.out@gmail.com (I. Outmani).

**Table 1**  
Chemical composition (wt%) of the three experimental alloys prepared for this study.

Alloys	Si	Cu	Mg	Zn	Fe	Mn	Ti	Ni	Cr, Pb, Sn	Al
Alloy A	9.64	3.23	0.4	1	0.82	0.15	0.04	0.06	< 0.04	bal.
Alloy B	9.75	1.44								
Alloy C	12.6	1.55								

properties of Al-Si alloys equivalent to the AlSi9Cu3 alloy. They concluded that increasing gate velocity (up to 80 m/s) and pressure (up to 61 MPa) reduce porosity and improve tensile properties. Concerning, the alloying elements content, Shabestari and Moemeni (2004) studied the influence of copper on microstructure and mechanical properties of AlSi7Cu3Mg0.4 alloy ( $x = 0.2; 0.7; 1.5; 2.5$ ). They observed that copper contributes to the formation of Al<sub>2</sub>Cu precipitates, which at the same time enhance the mechanical resistance of casting parts and the porosity. The influence of Si content was also examined by several authors (Wang et al. (1995), Kashyap et al. (1993) and Abdel-Jaber et al. (2010)) who pointed out that the increase of the Si content enhance the strength and hardness of the cast alloy but reduces its ductility.

Most of above studies investigate the effect of the alloying elements considering a unique given process condition. Few others deal with the effects of process parameters without taking care of the variability of alloying elements contents. Thus, the available literature studies do not approach the interactions occurring between both the alloys and processing parameters variabilities on the mechanical properties of cast parts.

## 2. Experimental procedure

A HPDC automotive support that keeps the powertrain in the car has been cast with different combinations of injection pressure, temperature of molten metal and chemical composition revealing the world variabilities.

### 2.1. Alloys studied

Alloying elements contents of the Al-Si-Cu alloys exhibits great variability in the world. The AlSi9Cu3 (Fe) alloy with a high content of Cu (3 wt%) is the most common in HPDC process in Europe. This alloy is known in USA as the A380 and its equivalents in Asia are ADC12

(Japan, China and India) with a lower content of Cu ( $\leq 2$  wt%) and AK12M2 (Russia) with higher content of Si (up 12.7 wt%) and lower content of Cu ( $\leq 2.5$  wt%).

To study the effect of the world variability of chemical composition (Si and Cu contents), three Al-Si-Cu alloys were selected: a hypo-eutectic alloy named A for considering the chemical composition of AlSi9Cu3 (Fe), a hypo-eutectic alloy named B and a near-eutectic alloy named C which represent respectively the ADC12 and the AK12M2 alloys (Table 1).

### 2.2. High pressure die casting and process parameters studied

The filling of the die cavity in HPDC occurs in three main stages (Fig. 1):

Stage I: this stage comprises filling the shot sleeve by molten metal and moving the plunger with a slow speed to limit turbulence of the metal.

Stage II: the die cavity is filled at high velocity to avoid premature solidification.

Stage III: Once the die cavity is full, high pressure is applied on the molten metal to prevent the formation of porosity during the solidification.

A mass of 300 kg melted at 700 °C was prepared using an electric resistance furnace; two casting temperatures were tested: 680 °C and 630 °C. The high tested temperature named HT (680 °C) is the same one used in HPDC for similar parts of AlSi9Cu3 (Fe) alloy, while the lower one named LT (630 °C) is chosen in order to evaluate the possibility to cast at low temperature by taking into account the conditions of castability of the three alloys. The molten metal temperature was controlled by using a holding furnace and then the melt was loaded into the shot sleeve of a 350 t HPDC machine for casting. All castings were performed with the same injection parameters except the pressure in stage III which control the injection pressure. Two different injection pressures were used: 87 MPa (named LP) and 127 MPa (HP). These injection pressures were oriented by ones used in automotive casting industry for similar compounds and by the capacity of the molding machine.

### 2.3. Characterization procedure

Tensile test specimens and hardness samples were extracted from several locations (1, 2, 3 and 4) of the casting pieces as shown in Fig. 2. Tensile tests were conducted following the NF EN ISO 6892-1 standard

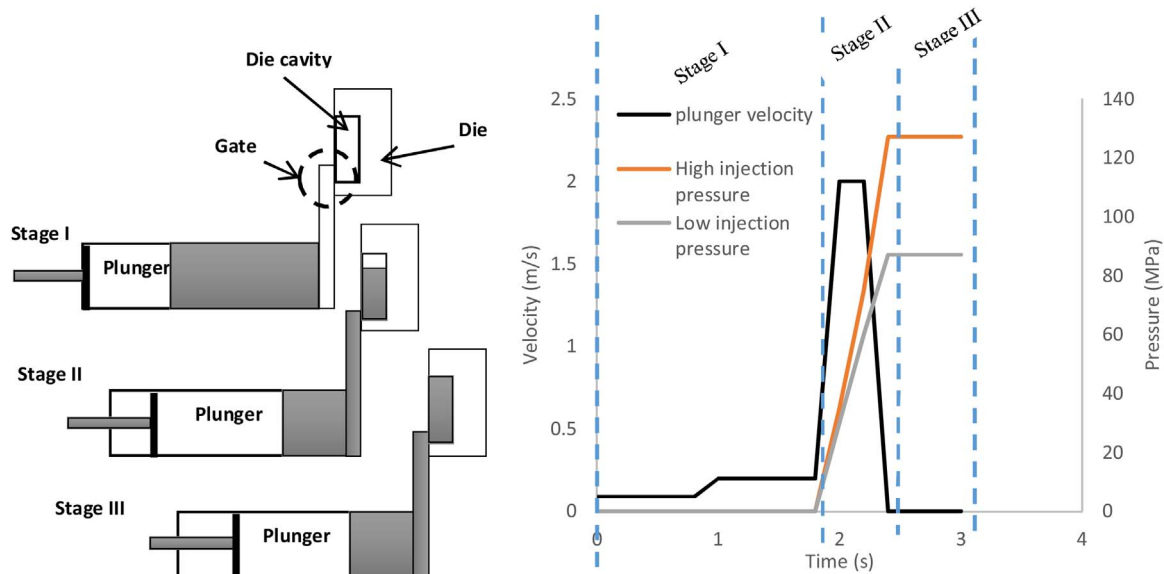


Fig. 1. Schematic description of the stages of HPDC process.

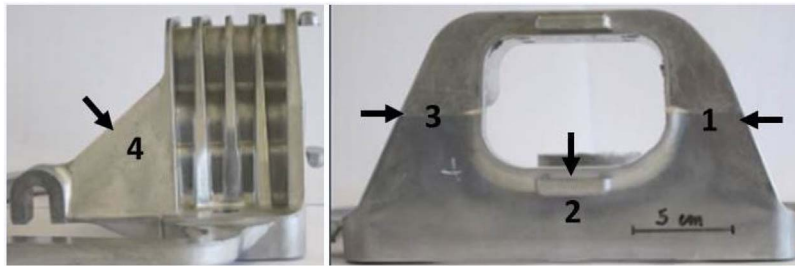


Fig. 2. Casting part and locations of samples for characterizations.

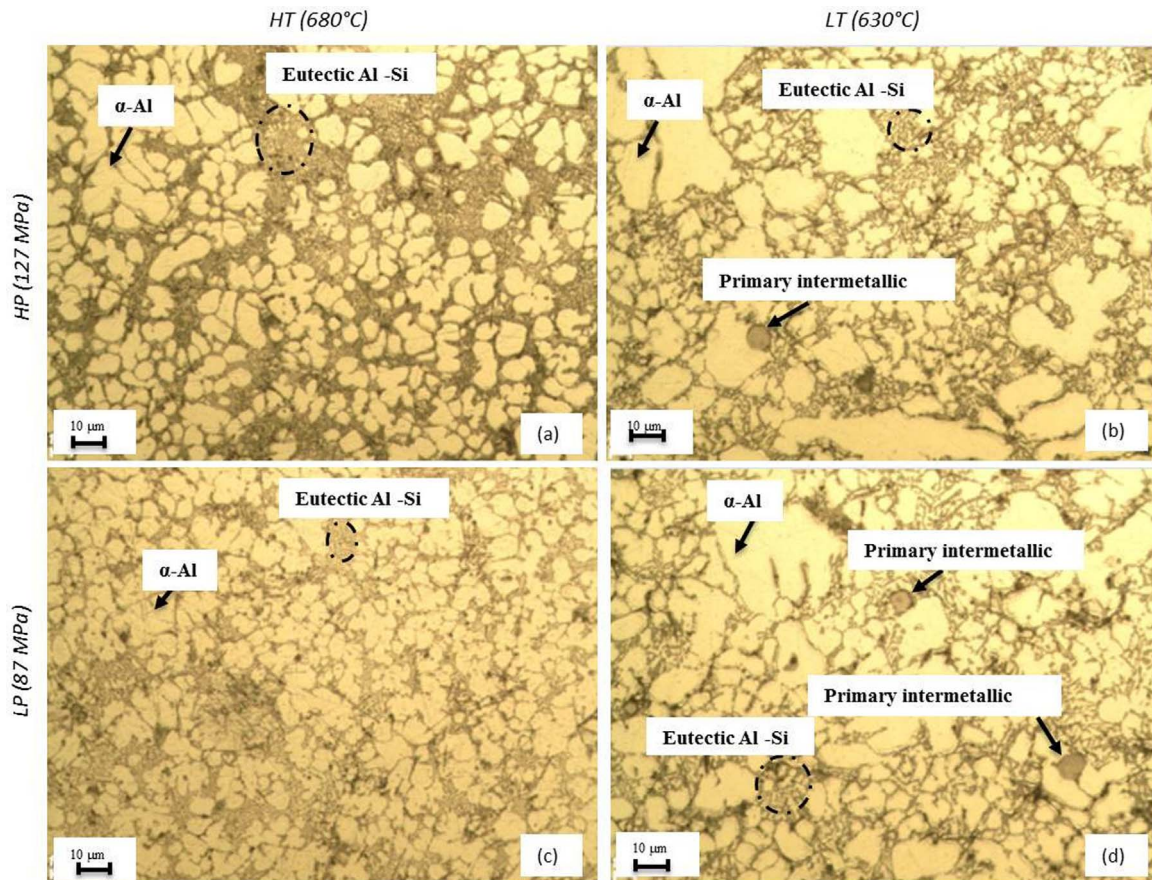


Fig. 3. OM micrographs of Alloy A injected at (a) 680 °C/127 MPa; (b) 630 °C/127 MPa; (c) 680 °C/87 MPa; (d) 630 °C/87 MPa.

using an INSTRON 4482 machine. All the tests were performed with a loading speed of 2 mm/min at ambient temperature. Tensile characteristics were calculated by taking the average of three testing. Brinell hardness measurements were conducted with a load of 0.6 kN and a tungsten carbide ball (diameter 2.5 mm). Each hardness value was calculated by taking the average of ten indentations.

Concerning metallographic observations, sample surface was prepared by a mechanical polishing up to 1  $\mu\text{m}$  followed by an etching with Keller solution (95 ml  $\text{H}_2\text{O}$ , 2.5 ml  $\text{HNO}_3$ , 1.5 ml  $\text{HCl}$  and 1 ml  $\text{HF}$ ) during 10–15 s. Microstructural features were obtained using an optical microscope (OM). SEM and EDS chemical mapping analyses were performed to observe and to identify the intermetallic compounds. Care was taken to guarantee adequate spatial resolutions for EDS quantification. Such that reliable quantification was only carried out for phases with sizes greater than 2  $\mu\text{m}$ . The percentage of porosity was evaluated using five OM images taken at the same magnification using the IMAGEJ software.

The effect of Si, Cu, temperature and pressure and their interactions on porosity level were studied through a statistical approach based on the analysis of variance (ANOVA). Each independent variable (Si, Cu, T

and P) was analyzed at two different levels, and a simplified model was carried out. For more detailed description of the statistical method used in this study we should refer to the work of Ferraro et al. (2015).

### 3. Results

#### 3.1. Microstructural observations

##### 3.1.1. General microstructure

The micrographs of the three alloys with different combinations of pressure and temperature are shown in Figs. 3–5. All the Al-Si-Cu alloys exhibit in a various proportion a primary  $\alpha$ -Al dendritic phase (light phase), an eutectic inter-dendritic Al-Si phase (dark phase) and inter-metallic compounds identified in a further paragraph.

For the both hypo-eutectic alloys A and B, the  $\alpha$ -Al dendritic phase (Figs. 3(a) and 4(a)) obtained at high temperature of injection is smaller and more homogeneous than dendrites observed at low temperature (Figs. 3(b) and 4(b)). Furthermore, the Al-Si phase displays a fibrous morphology for these alloys (Figs. 3(a) and 4(a)) to a plate-like one (Fig. 5(a)) for the alloy C. SEM highlights this observation on Fig. 6.



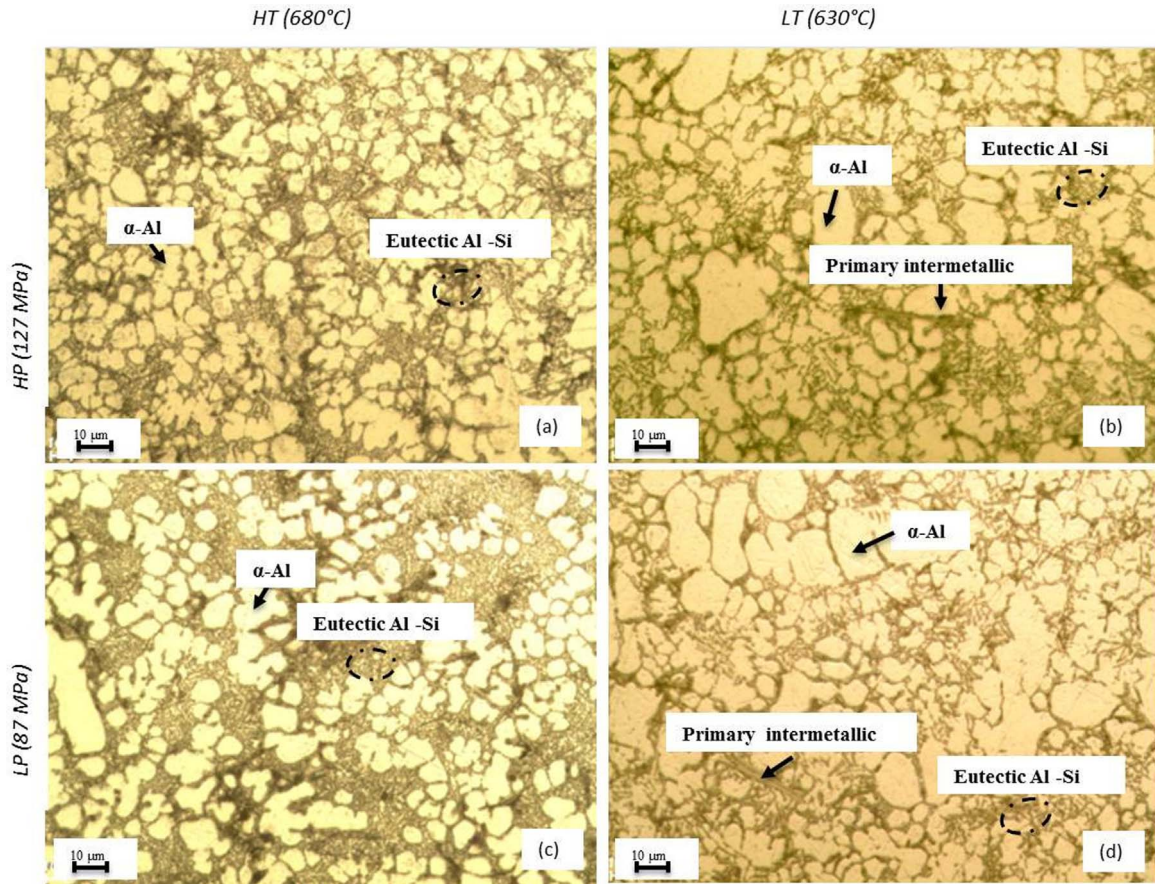


Fig. 4. OM micrographs of Alloy B injected at (a) 680 °C/127 MPa; (b) 630 °C/127 MPa; (c) 680 °C/87 MPa; (d) 630 °C/87 MPa.

Comparing micrographs (a) and (c) of Figs. 3 and 4, high pressure in stage III seems to promote a finer and more fragmented microstructure: smaller dendrites and higher fractions of the Al-Si eutectic phase are observed when the high injection pressure is applied (HP). But, the effect of injection temperature is predominant, especially for the alloy A.

On the opposite, the different processing parameters seem have no effect on the microstructural features of the near eutectic alloy C, except for the presence of large primary Si particles noted on the micrographs (b) and (d) of Fig. 5 for low temperature (LT).

### 3.1.2. Intermetallic compounds

Intermetallic compounds are observed within the three cast alloys tested, whatever the processing parameters applied, but EDS analysis were only performed at low temperature when the coarsest intermetallic compounds are detected (micrographs (b) and (d) of Figs. 7–9).

As listed in Table 2, for the both hypo-eutectic alloys A and B, coarse compounds with polyhedral morphology are observed (noticed ① on Figs. 7 and 8) with a notable lower amount for the alloy B than A.

The chemical analysis (Table 3) shows that such a precipitate is the well-known Fe-rich  $\alpha\text{-Al}_{15}(\text{Fe}, \text{Mn})_3\text{Si}_2$  phase and reveals that the  $\alpha\text{-Al}_{15}(\text{Fe}, \text{Mn})_3\text{Si}_2$  phase contains Cu directly related to the own Cu content of the alloy: 3.02 for alloy A versus 1.04 for B. The Cu element, as a transition metal, is known to stabilize the  $\alpha\text{-Al}_{15}(\text{Fe}, \text{Mn})_3\text{Si}_2$  phase and to promote its development (Mondolfo, 1976). Small polyhedral  $\alpha\text{-Fe}$  compounds are observed in alloys A and B too (details in Fig. 10(c)). As mentioned by Bäckerd et al. (1990), unlike to the coarse Fe-rich  $\text{Al}_{15}(\text{Fe}, \text{Mn})_3\text{Si}_2$  phases, these intermetallic compounds are formed after the development of the dendrites. No chemical analysis was done on these micrometric particles.

Regarding the alloy C, the intermetallic compounds formed are

coarse needle shaped (Fig. 9 and Table 2). EDS analysis (Table 3) shows that they are the well-known  $\beta\text{-AlFeSi}$  precipitates. It should be note that the three alloys tested contain small particles of  $\beta\text{-AlFeSi}$  detailed in Fig. 10(a) but their small size does not permit to carry out EDS analysis.

At last, intermetallic compounds noticed ② are observed in the three alloys tested. They are the well-known  $\theta\text{-Al}_2\text{Cu}$  phase (Table 3). As detailed on Fig. 10(b), these Cu-rich compounds are localized in the interdendritic spaces because they are formed at the end of the solidification. The alloy A contains the largest amount of these compounds, in accordance with its own highest Cu content.

### 3.1.3. Porosity defects

The Fig. 11 shows the porosity (shrinkage + gas) area percentage as a function of temperature for the two injection pressures, (a) at 127 MPa and (b) at 87 MPa. Comparing the results for the three alloys tested, one can notice that at high pressure and temperature, the porosity levels are the lowest but the alloy A has the highest values. Moreover, the reduction of both casting pressure and temperature promotes porosity.

As highlighted by optical micrographs (d)–(f) in Fig. 12, the temperature decrease provides a more important number of blank spaces with irregular shape. This leads to conclude that decreasing temperature promotes shrinkage cavities.

The temperature reduction increases dramatically the porosity level whatever the pressure tested. This tendency especially affects the alloy C (+173% at 127 MPa and +87% at 87 MPa).

Concerning the influence of pressure, it is noticed, through the comparison of the OM images (g)–(i) in Fig. 12 that the number of pore nucleation sites does not increase with decreased pressure. However, the pore size, and hence the amount of porosity increases. This is



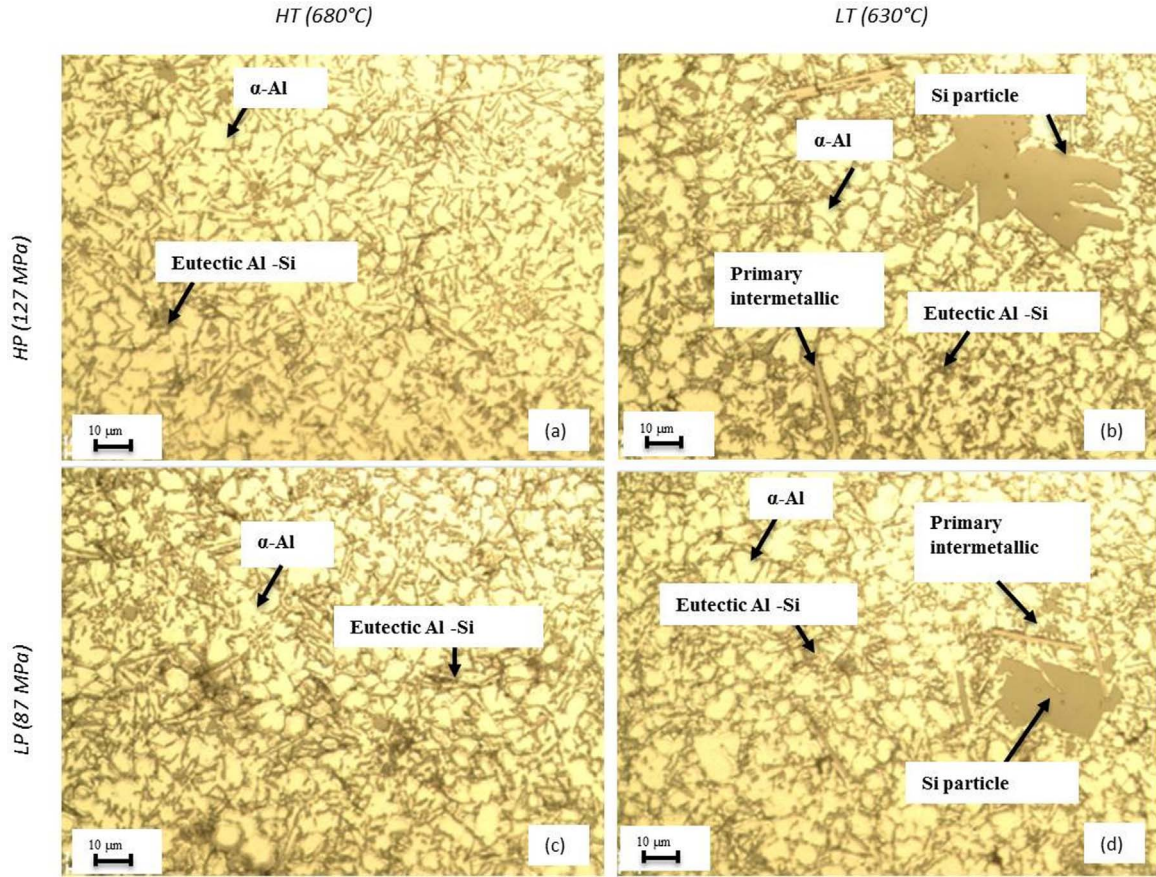


Fig. 5. OM micrographs of Alloy C injected at (a) 680 °C/127 MPa; (b) 630 °C/127 MPa; (c) 680 °C/87 MPa; (d) 630 °C/87 MPa.

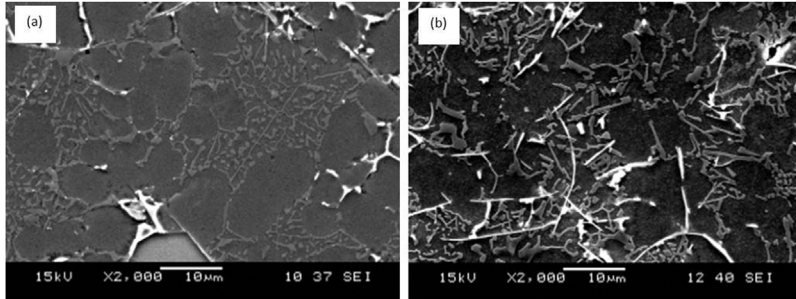


Fig. 6. Details of Al-Si phase morphology for (a) hypo-eutectic (A or B), (b) near-eutectic (C) alloys.

confirmed by comparing Fig. 11(a) and (b) and suggests that the decrease in pressure increases the size of gas porosity.

At low temperature, the decrease in pressure increases the porosity level of the three alloys: +25% for alloy A, +29% for alloy C and +50% for alloy B. However, at high temperature, the same decrease in pressure increases the porosity level for the alloys B and C respectively by +68% and +83%, but has no effect on the alloy A. This may be due to the large amount of  $\theta$ -Al<sub>2</sub>Cu Cu-rich intermetallics in this alloy which may limit the growth of porosity (Fig. 13).

The results of the analysis of variance (ANOVA) implemented to investigate the effect of varied alloying elements (Cu and Si), injection temperature and pressure on the area of porosity are shown on the Table 4 and Fig. 14. This figure indicates that the temperature (percentage of contribution, PC = 42%), the pressure (PC = 23%) and the Cu content (PC = 13%) have statistical and physical significance on the porosity formation. This statistical analysis has also highlighted that the interaction between the Si content and the injection temperature assists on the porosity formation with a percentage of contribution of 15%.

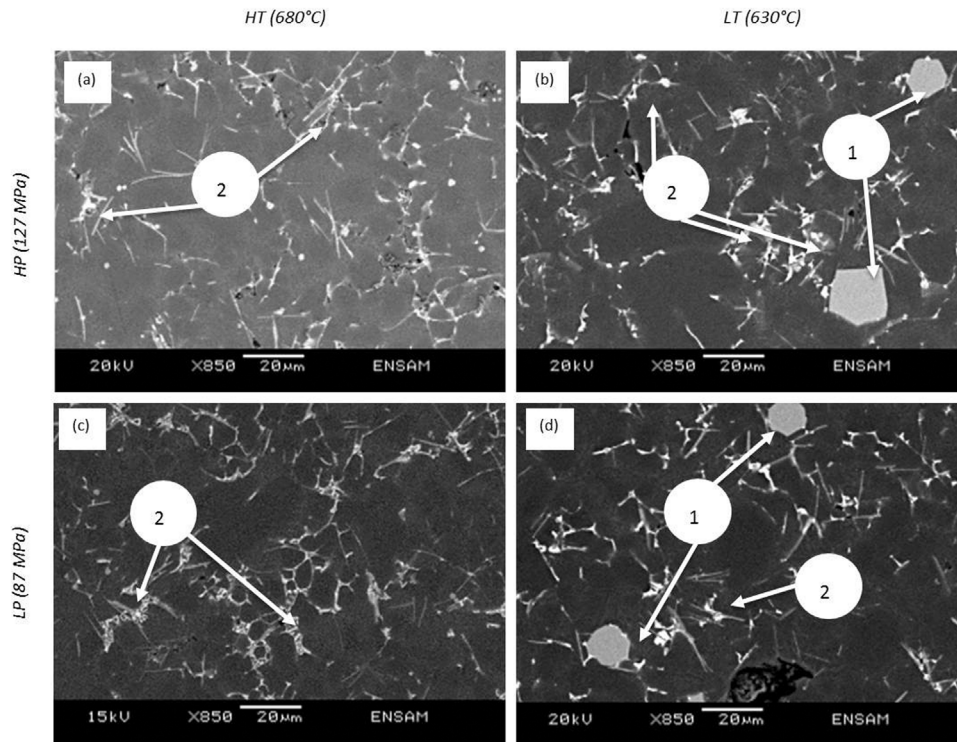
### 3.2. Mechanical properties

#### 3.2.1. Tensile characteristics

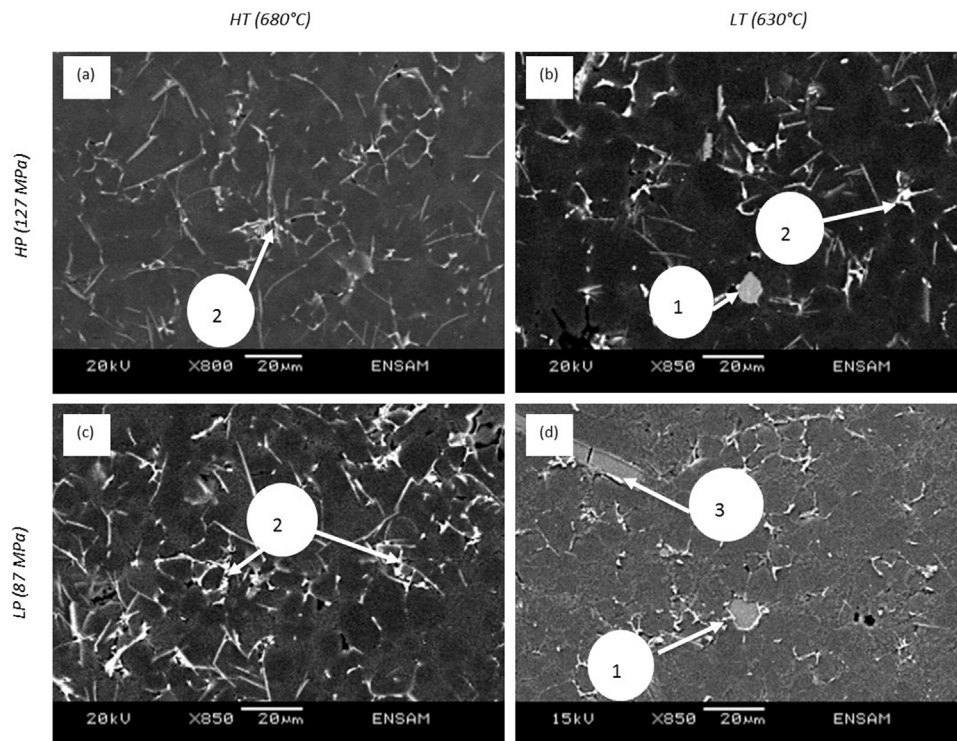
For the three alloys tested, the variations of YS, UTS and e% are respectively shown in Figs. 15–17 as a function of temperature for the two pressures.

Fig. 15(a) shows that at both high pressure and temperature, the three alloys have the highest tensile strength: the both hypo-eutectic alloys A and B have almost the same values of YS (~150 MPa) and UTS (near 230 MPa) while the near-eutectic C alloy has a lower YS (136 MPa). For the two temperatures tested, YS does not change for the alloys A and B with pressure reduction or decreases only by 7% for the alloy C.

Concerning UTS, the both hypo-eutectic alloys A and B have again the highest and almost the same values (230 MPa) when both temperature and pressure are maximum (HT and HP). At high pressure, this property decreases (17%, 15%, and 9% for alloy B, A and C respectively) with decreasing temperature, but the simultaneous reduction of temperature and pressure reduces UTS (14% for the alloy B and 9% for



**Fig. 7.** SEM micrographs of intermetallic compounds in alloys A injected at (a) 680 °C/127 MPa; (b) 630 °C/127 MPa; (c) 680 °C/87 MPa; (d) 630 °C/87 MPa.



**Fig. 8.** SEM micrographs of intermetallic compounds in alloys B injected at (a) 680 °C/127 MPa; (b) 630 °C/127 MPa; (c) 680 °C/87 MPa; (d) 630 °C/87 MPa.

the alloys A and C) as seen in Fig. 16.

The slight variation and the large dispersions of  $e\%$  in Fig. 17 do not allow identifying the influence of alloying elements and process parameters on this property.

In summary, the alloy A differentiates from B and C with higher tensile strength and improved resistance under a combination of high temperature and pressure (HT and HP).

### 3.2.2. Hardness

Concerning hardness, at high pressure and high temperature (Fig. 18), the alloy A shows the highest value of hardness. On the contrary, the alloy B has the lowest hardness. This is due to the high content of Cu which promotes the formation of the Cu-rich intermetallic  $Al_2Cu$ . The near-eutectic alloy C has a better hardness than the alloy B. These both alloys have the same Cu content but the alloy C has a higher Si content than B.

The effect of the injection temperature on the hardness at the both



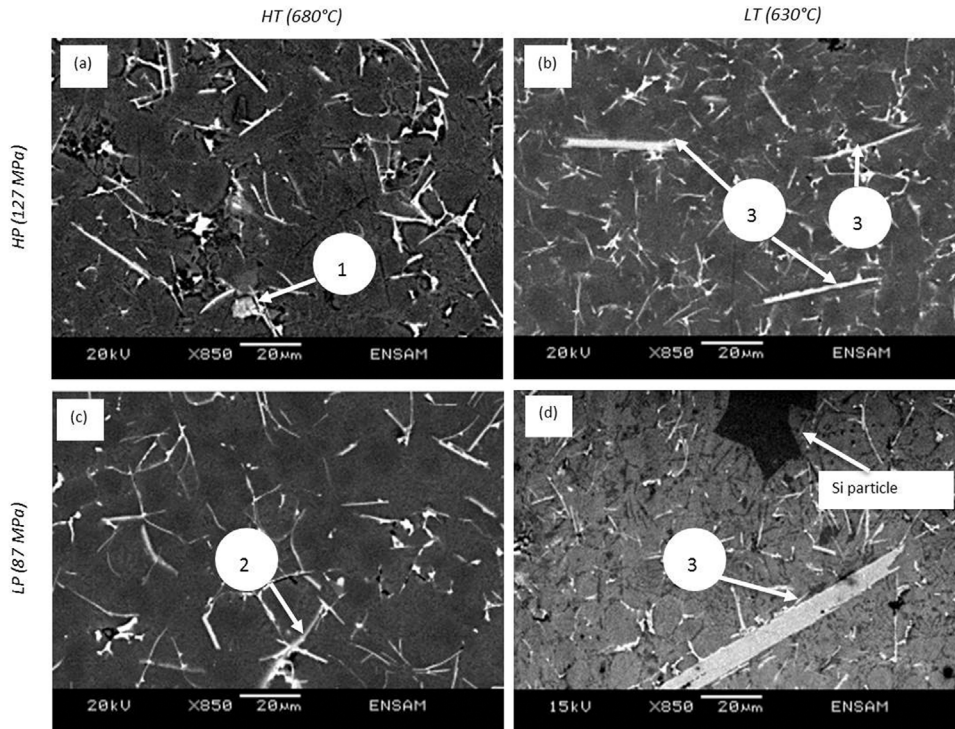


**Fig. 9.** SEM micrographs of intermetallic compounds in alloys C injected at (a) 680 °C/127 MPa; (b) 630 °C/127 MPa; (c) 680 °C/87 MPa; (d) 630 °C/87 MP.

**Table 2**  
Intermetallic compounds detected in alloys A, B and C.

Alloy	Compound	Morphology and color
A	①	Coarse hexagon-shaped, grey
	②	Block-like, white
B	①	Coarse hexagon-shaped, grey
	②	Block-like, white
	③	Coarse Needle-shaped, dark grey
C	②	Block-like, white
	③	Coarse Needle-shaped, dark grey

pressures is shown in Fig. 18. There was no significant change with the variation of temperature and pressure.

#### 4. Discussion

##### 4.1. Influence of process parameters

The injection pressure changes the microstructure of aluminum alloys Al-Si: as previously seen, a high pressure provides more fragmented dendrites of the  $\alpha$ -Al phase and more homogenous microstructure for hypo-eutectic alloys. According to Santos et al. (2015), the microstructural refinement caused by fragmentation of primary aluminum dendrites, may enhance mechanical properties (hardness, YS

UTS and e%).

At low pressure for the three alloys studied in this work, the highest level of porosity is obtained. As confirmed by Dargusch et al. (2006), the main purpose of application pressure in HPDC process is to limit entrapment of gas bubbles and shrinkage of the molten due to the turbulent flow during the solidification.

The temperature of the molten metal plays an important role on the formation of intermetallic compounds. Principal Fe-intermetallic in Al-Si-Fe alloys is reported to be:  $\beta$ -AlFeSi (needles) and  $\alpha$ -AlFeMnSi (sludges) (Taghiabadi et al., 2008). These phases, particularly needles act as stress raisers and contribute to the brittleness of the cast parts. The polyhedral  $\alpha$ -AlFeMnSi phase is considered less harmful to the mechanical properties compared to the needle-like  $\beta$ -AlFeSi phase. Thus, altering  $\beta$ -AlFeSi into  $\alpha$ -AlFeMnSi is advantageous from the point of view of mechanical properties. The casting and holding temperatures of the liquid metal has been studies in the literature by Shabestari (2004). According to this author, Fe-rich intermetallic compounds have high melting points and if the metal is maintained in the furnace at low temperature; the Fe-rich intermetallic compounds crystallize and grow in the liquid metal before casting. Because of their high density, they drop into the bottom of the bath and if they are pulsed, they are found in the casting. These compounds act as hard points and reduce the mechanical properties of casting parts. Shabestari (2004) reported that the Fe-intermetallic temperature formation depends on the Fe content according to the formula  $T (^{\circ}\text{C}) = 645.7 + 34.2 (\% \text{Fe})^2$ . For our three alloys, with the  $\% \text{Fe} = 0.82\%$ ,  $\alpha$ -Fe-intermetallic compounds form

**Table 3**  
Quantitative EDS results of intermetallic compounds.

Intermetallic compounds	Alloy	Element (% at)									Phase	Suggested formula
		Al	Si	Fe	Mn	Cu	Cr	Zn	Ni	Mg		
①	A	70.2	12.1	10.1	3.8	3.02	0.3	0.2	0.28	0	Primary Fe-rich $\alpha$ phase	$\alpha$ -Al <sub>15</sub> (Fe, Mn) <sub>3</sub> Si <sub>2</sub>
	B	71	12.9	10.68	3.75	1.04	0.24	0.2	0.15	0		
②	A, B, C	69.1	2.25	0.1	0.01	26.3	0	1.5	0.7	0.08	Cu-rich phase	Al <sub>2</sub> Cu
③	B	66.3	20.6	11.47	1.03	0.15	0.01	0.11	0.36	0	Primary Fe-rich $\beta$ phase	$\beta$ -Al <sub>5</sub> FeSi
	C	65.3	20.2	11.6	1.23	0.82	0	0.16	0.65	0.04		



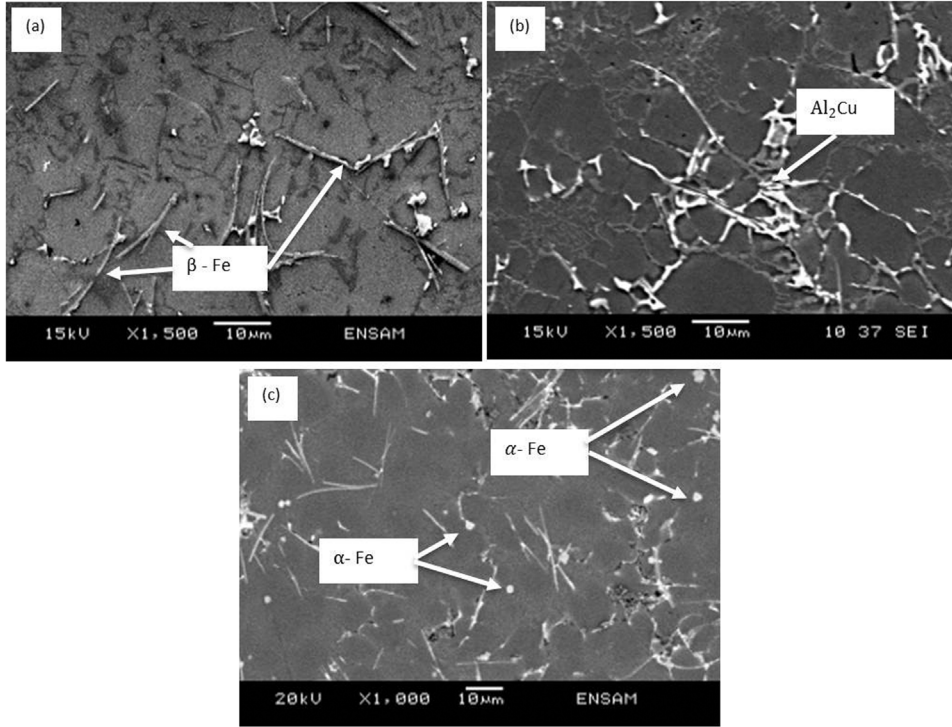


Fig. 10. SEM details of (a) co-eutectic  $\beta$ -Fe compounds, (b)  $\text{Al}_2\text{Cu}$  precipitates, (c) post-dendritic  $\alpha$ -Fe compounds.

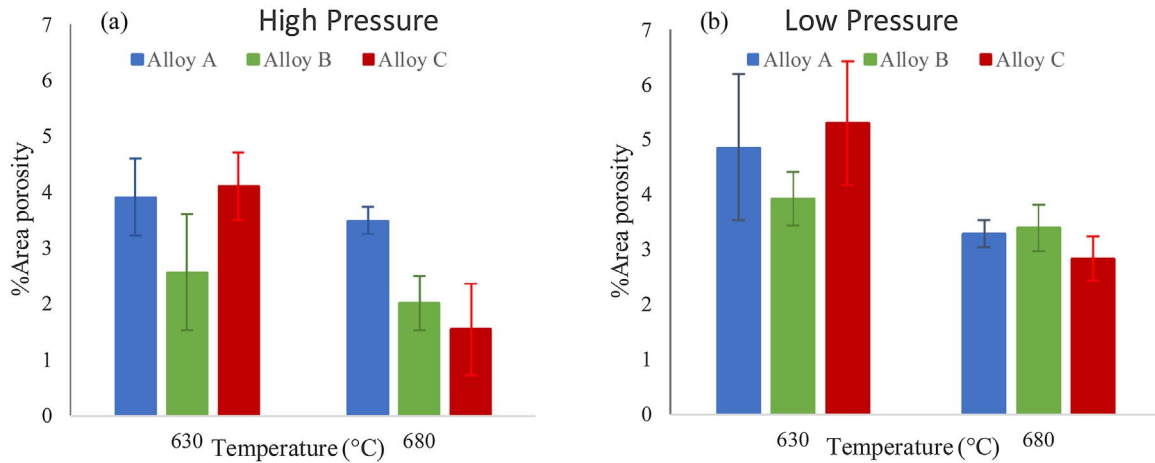


Fig. 11. Effect of temperature on porosity area percentage (a) at high pressure (HP): 127 MPa and (b) at low pressure (LP): 87 MPa.

since 668 °C. This is in agreement with the presence of coarse Fe-rich compounds at only low temperature (630 °C) as previously noticed. The results of the investigation of the influence of the casting temperature on porosity detailed in the paragraph 3.1.3 show that casting temperature has also a significant influence on the formation of porosity promoting more shrinkage porosity. With increasing the temperature of the molten metal and due to higher heat content, the alloy remains in liquid state for a longer duration and therefore the liquid metal is available to compensate the normal solidification shrinkage as maintained by Ma (2002). On the other hand, Ma et al. (2008) reported that large Fe-rich compounds which form early in the solidification process, tend to restrict liquid metal feeding and may cause the formation of shrinkage porosity during the casting process.

To conclude, high pressure (127 MPa) and high temperature (680 °C) are the optimum values to reduce the density of porosity.

#### 4.2. Influence of alloying elements

Cu forms with aluminum the intermetallic  $\text{Al}_2\text{Cu}$  which precipitates at the end of the solidification through the ternary eutectic reaction  $\text{liq} \rightarrow \alpha\text{-Al} + \text{Si} + \text{Al}_2\text{Cu}$  as stated by Shabestari and Moemeni (2004). These Cu-rich phases (detailed in Fig. 9(a)) contribute to strengthening the casting. Thus, a significant improvement was obtained for the YS and UTS of the alloy A that contains 3.3% of Cu. On the other hand, Cu increases the porosity content of A. Indeed,  $\text{Al}_2\text{Cu}$  phases solidify at very low temperatures, which do not allow filling them completely and therefore facilitates the formation of the micro-porosity according to Caceres et al. (1999). This is well consistent with the results obtained by Shabestari and Moemeni (2004) who noticed that a Cu content exceeding 2.5% reduces the eutectic temperature which increases the solidification range and therefore promotes the porosity formation.

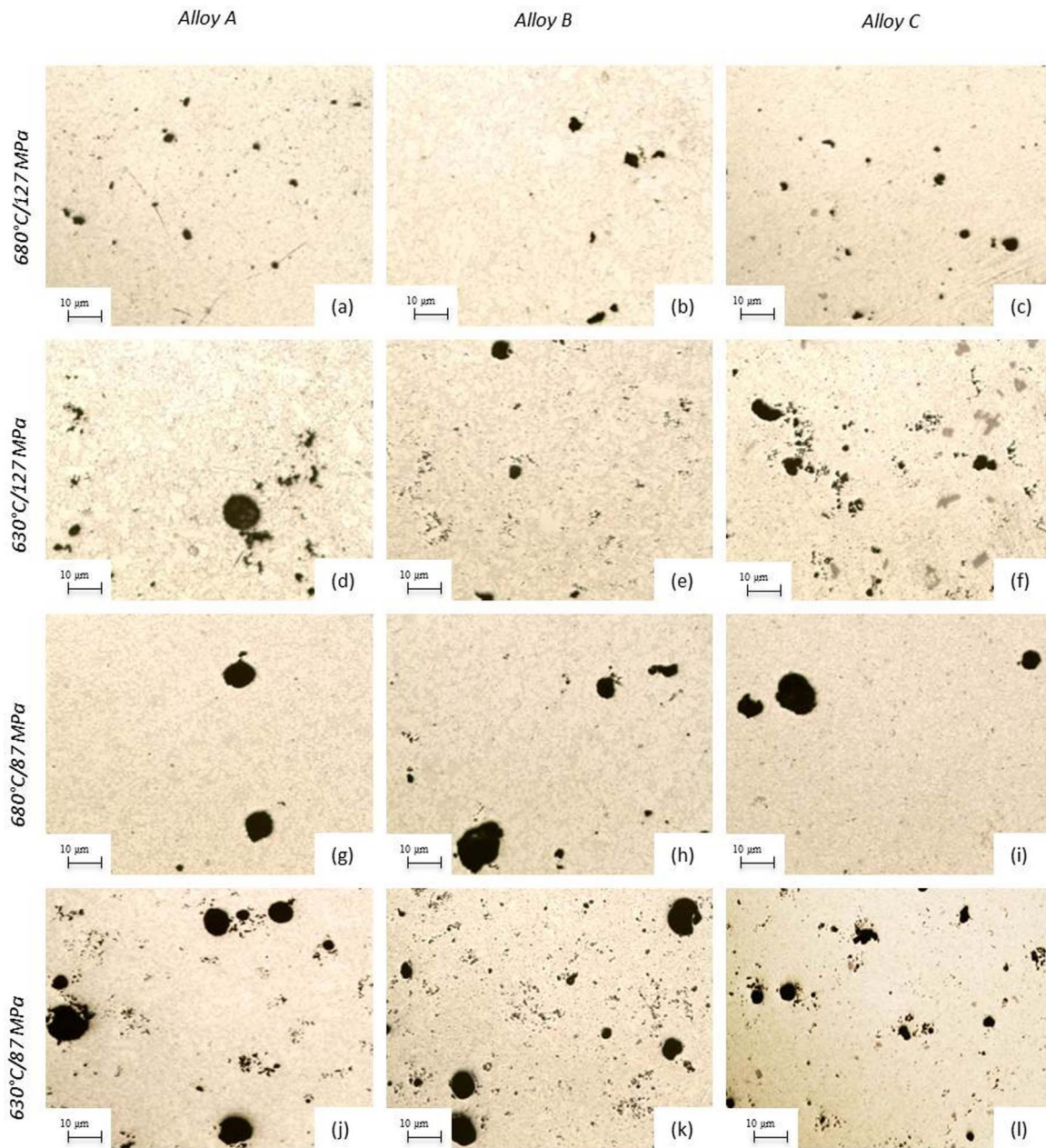


Fig. 12. Optical micrographs of porosity in Alloys A, B and C.

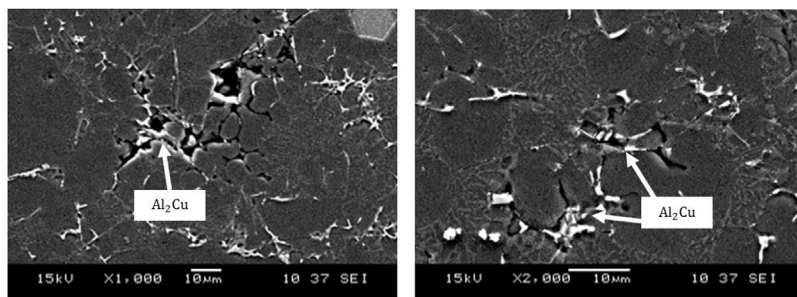


Fig. 13. Cu-rich phases in alloy A at low pressure.

It has been shown (paragraph 3.3) that the raise of the Si content increases the fraction of eutectic phase to the detriment of the  $\alpha$ -Al. This deteriorates the YS and the UTS and promotes the formation of Fe-rich intermetallic compounds  $\beta$ -AlFeSi (as seen in Fig. 9 for C). Larger amounts of eutectic liquid ensure enough space and time for the growth of the intermetallics, hence their size keep going up. A high Si content

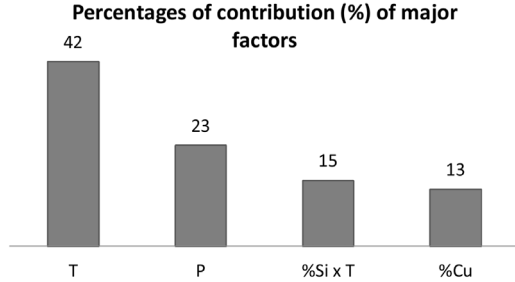
also increases the fraction and the size of Si particles (Fig. 9d). According to Grosselle et al. (2009), these particles play an undoubted role in the fracture behavior of Al-Si alloys. A reduction of the mechanical properties (especially UTS and elongation to fracture) is observed when the size of Si particles increases, Si particles leading to high tension field around these particles. This promotes cleavage



**Table 4**

ANOVA table for the porosity area.

Source of variance	Degree of freedom	Sum of Squares	Significance level $\alpha$	F-Test	P-Value	Percentage of contribution (%)
T	1	5.454	0.05	44.531	0.022	42
P	1	2.956	0.05	24.132	0.039	23
%Cu	1	1.662	0.05	13.569	0.04	13
%Si	1	0.001	0.05	0.006	0.946	0
%Si $\times$ T	1	2.029	0.05	16.562	0.048	15
%Si $\times$ P	1	0.094	0.05	0.768	0.473	1
%Cu $\times$ T	1	0.101	0.05	0.827	0.459	1
%Si $\times$ %Cu	0	0.000	0.05	–	–	0
Error	2	0.245	0.05	–	–	5
Total	9	13.124	0.05	–	–	100

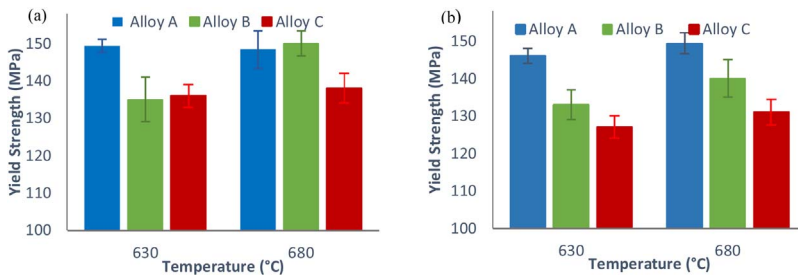
**Fig. 14.** Contributions of influential factors on the variation of porosity area.

mechanism and thus, fracture can easily propagate. The low tensile characteristics obtained for the alloy C in which a large number of Si particles is observed can be therefore understood.

#### 4.3. Influence of interaction between alloying elements and process parameters

The effect of pressure on the formation of porosity can be directly related with the alloying elements content. For both a high content of silicon and a low one of Cu (Alloy C), the decrease of pressure raises significantly the rate of porosity unlike for the high Cu content (Alloy A). In fact, if the pressure decrease essentially improves the size of porosity, the  $\text{Al}_2\text{Cu}$  phases that formed at the end of solidification may limit its growth.

Copper has another effect on the microstructural changes that enhance the tensile properties (YS and UTS): in the Alloy A, Cu promotes the formation of  $\alpha\text{-AlFeMnSi}$  phases instead of  $\beta\text{-AlFeSi}$  phases, which is in accordance with the results of Fang et al. (2007). The decrease in temperature result in the formation of intermetallic compounds (Figs. 7, 8 and 9) as the temperature of formation of these compounds (668 °C) is reached while the liquid metal is maintained in the furnace before casting. But, the Fe-intermetallic observed in alloy A which contain 3.3% of Cu are  $\alpha\text{-AlFeMnSi}$  while those observed in the alloys C with a low Cu content are  $\beta\text{-AlFeSi}$  needle shaped. This is in agreement with the low values of YS (~135 MPa) obtained for the alloys B and C compared to that (152 MPa) of alloy A at low temperature.

**Fig. 15.** Effect of temperature on YS (a) at 127 MPa and at (b) 87 MPa.

Silicon and injection temperature interaction has a significant effect on the formation of porosity. Indeed, increasing both the silicon content and the injection temperature decreases the porosity level (the lowest porosity level (1.54%) is obtained for the alloy C at HT). This is confirmed by 15% of contribution for the interaction between Si and injection temperature (%Si  $\times$  T).

#### 5. Conclusions

In the present work, the influence of chemical composition, casting temperature, injection pressure and the interaction between the tested alloying elements and the tested process parameters on mechanical properties and microstructural features of die cast aluminum parts was investigated. In accordance with the results of the ANOVA, we can conclude that:

- High Cu content contributes to the formation of  $\text{Al}_2\text{Cu}$  phases, which improve mechanical properties.
- High Si content favors the formation of  $\beta\text{-AlFeSi}$  needle-shaped particles.
- Low injection temperature promotes the formation of coarse Fe rich intermetallics. However, the type and the shape of these compounds are influenced by Si and Cu contents.
- Cu further promotes the polyhedral morphology of Fe-rich phases ( $\alpha\text{-AlFeMnSi}$ ). Thus, high Cu content reduces the effect of temperature unlike high Si content increases it. High content of Cu indeed makes the  $\text{AlSi9Cu}$  alloy (used in Europe with 3 wt% Cu) less sensitive to degradation of the casting temperature in comparison with low Cu alloys (for example ADC12 used in Asia).
- Decreasing casting temperature and injection pressure promotes porosity rate in casting parts. The size of gas-porosity can be limited by the precipitation of inter-dendritic compounds  $\text{Al}_2\text{Cu}$  at the end of the solidification (alloy A).
- For hypo-eutectic alloy (A or B), the combination of higher temperature and pressure provides smaller and more globular  $\alpha\text{-Al}$  surrounded by Al-Si eutectic phases unlike near-eutectic alloy (C) for which a unique microstructure was observed for the different values of processing parameters.

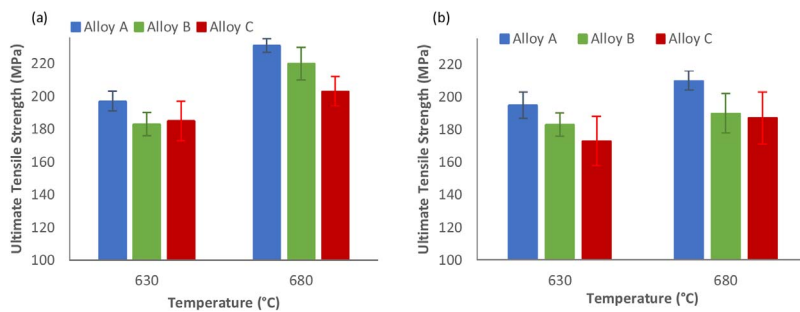


Fig. 16. Effect of injection temperature on UTS (a) at 127 MPa and (b) at 87 MPa.

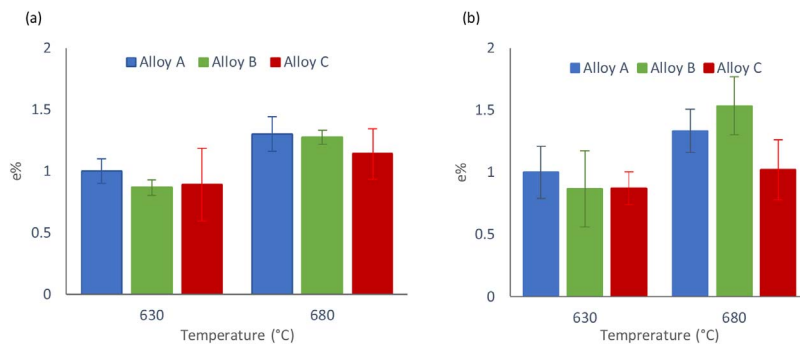


Fig. 17. Effect of injection temperature on e% (a) at 127 MPa and (b) at 87 MPa.

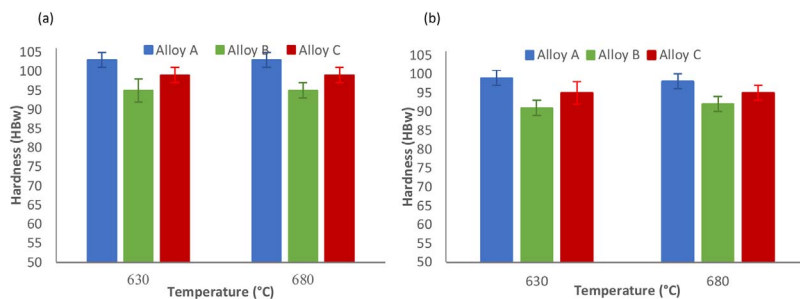


Fig. 18. Effect of injection temperature on Hardness (a) at 127 MPa and (b) at 87 MPa.

## Acknowledgements

The authors express their grateful acknowledgement for financial support received from RENAULT. Sincere thanks also due to Ms A. Huguet for the technical discussion, Mr. D. Colombi and Mr J. Voisin for their valuable technical assistance.

## References

- Abdel-Jaber, G.T., Omran, A.M., Abdelrazek Khalil, K., Fujii, M., Seki, M., Yoshida, A., 2010. An investigation into solidification and mechanical properties behavior of Al-Si casting alloys. *Int. J. Mech. Mechatron. Eng.* 10 (04), 30–35.
- Adamane, A.R., Arnberg, L., Fiorese, E.E., Timelli, G., Bonollo, F., 2015. Influence of injection parameters on the porosity and tensile properties of high-pressure die cast Al-Si alloys: a review. *Am. Foundry Soc.* 9, 43–53.
- Ashiri, R., Niroumand, B., Karimzadeh, F., Hamani, M., Pouranvari, M., 2009. Effect of casting process on microstructure and tribological behaviour of LM13 alloy. *J. Alloys Compd.* 475, 321–327.
- Ashiri, R., Karimzadeh, F., Niroumand, B., 2014. On effect of squeezing pressure on microstructural characteristics, heat treatment response and electrical conductivity of an Al-Si-Mg-Ni-Cu alloy. *Mater. Sci. Technol.* 30, 1162–1169.
- Bäckerud, L., Chai, G., Tamminen, J., 1990. Solidification characteristics of aluminum alloys. *Foundry Alloys* 2.
- Caceres, C.H., Djurdjevic, M.B., Stockwell, T.J., Sokolowski, J.H., 1999. The effect of Cu content on the level of microporosity in Al-Si-Cu-Mg casting alloys. *Scripta Mater.* 40 (5), 631–637.
- Dargusch, M.S., Dour, G., Schauer, N., Dinnis, C.M., Savage, G., 2006. The influence of pressure during solidification of high pressure die cast aluminium telecommunications components. *J. Mater. Process. Technol.* 180, 37–43.
- Fang, X., Shao, G., Liu, Y.Q., Fan, Z., 2007. Effects of intensive forced melt convection on the mechanical properties of Fe containing Al-Si based alloys. *Mater. Sci. Eng. A* 65–72.
- Ferraro, S., Fabrizio, A., Timelli, G., 2015. Evolution of sludge particles in secondary die-cast aluminum alloys as function of Fe, Mn and Cr contents. *Mater. Chem. Phys.* 153, 168–179.
- Grosselle, F., Timelli, G., Bonollo, F., Molina, R., 2009. Correlation between microstructure and mechanical properties of Al-Si diecast engine. *Metall. Sci. Technol.* 27–2, 2–10.
- Kashyap, K., Murali, S., Raman, K., Murthy, K., 1993. Casting and heat treatment variables of Al-7Si-Mg alloy. *J. Mater. Sci. Technol.* 9, 18–204.
- Ma, Z., Samuel, A.M., Samuel, F.H., Doty, H.W., Valtierra, S., 2008. A study of tensile properties in Al-Si-Cu and Al-Si-Mg alloys: effect of  $\beta$ -iron intermetallics and porosity. *Mater. Sci. Eng. A* 490, 36–51.
- Ma, Z., 2002. Effect of Fe-intermetallics and Porosity on Tensile and Impact Properties of Al-S-Cu and Al-Si-Mg Cast Alloys. Quebec University.
- Mondolfo, L.F., 1976. *Aluminum Alloys: Structure and Properties*, first ed. Butterworths, London.
- Obiekea, K.N., Aku, S.Y., Yawas, D.S., 2014. Effects of pressure on the mechanical properties and microstructure of die cast aluminum A380 alloy. *J. Miner. Mater. Charact. Eng.* 2, 248–258.
- Santos, S.L., Antunes, R.A., Santos, S.F., 2015. Influence of injection temperature and pressure on the microstructure mechanical and corrosion properties of a AlSiCu alloy processed by HPDC. *Mater. Des.* 88, 1071–1081.
- Shabestari, S.G., Moemeni, H., 2004. Effect of copper and solidification conditions on the microstructure and mechanical properties of Al-Si-Mg alloy. *J. Mater. Process. Technol.* 193–198.
- Shabestari, S.G., 2004. The effect of iron and manganese on the formation of intermetallic compounds in aluminum-silicon alloys. *Mater. Sci. Eng. A* 383, 289–298.
- Taghiabadi, R., Ghasemi, H.M., Shabestari, S.G., 2008. Effect of iron-rich intermetallics on the sliding wear behavior of Al-Si alloys. *Mater. Sci. Eng. A* 490, 162–170.
- Timelli, G., Bonollo, F., 2008. Quality mapping of aluminium alloy diecastings. *Metall. Sci. Technol.* 26–1, 2–8.
- Timelli, G., Bonollo, F., 2010. The influence of Cr content on the microstructure and mechanical properties of AlSi9Cu3 (Fe) die-casting alloys. *Mater. Sci. Eng. A* 528, 273–282.
- Wang, L., Makhlof, M., Apelian, D., 1995. Aluminium die casting alloys: alloy composition, microstructure and properties-performance relationships. *Int. Mater. Rev.* 40, 221–238.